VOL. 17, NO. 12, JUNE 2022 ISSN 1819-6608
ARPN Journal of Engineering and Applied Sciences

www.arpnjournals.com

PARTICLE MOTION IN JIGS USING LINEAR AND NONLINEAR EMPIRICAL MODELS

Manuel A. Ospina-Alarcón[1], Liliana M. Úsuga-Manco[2] and Gabriel E. Chanchí-Golondrino[1]
[1]Ingeniería de Sistemas, Facultad de Ingeniería, Universidad de Cartagena, Cartagena, Colombia
[2]Departamento de Educación y Ciencias Básicas, Facultas de Ciencias Exactas y Aplicadas, Instituto Tecnológico Metropolitano, Medellín, Colombia
E-Mail: mospinaa@unicartagena.edu.co

ABSTRACT

Particle properties can have a great influence on the design, optimization, and control of plants in the processing of heavy minerals such as gold and silver. In this paper, the identification of the position of a particle in the bed of a Jig-type gravity concentrator was proposed by means of data obtained from a phenomenological model of the particle trajectory. The data obtained from the phenomenological model were used for the construction and validation of an auto-regressive model with exogenous input (ARX) and an artificial neural network (ANN) model. The results obtained were contrasted and the construction process of both models was documented. The identified models showed a fit with errors lower than 2 % with respect to the data provided by the phenomenological model, which makes them suitable for control and optimization purposes of the equipment in mineral recovery.

Keywords: dynamic systems identification, mineral processing, empirical modeling, ARX models, gravimetric concentration.

INTRODUCTION

The use of models in the mineral processing industry is becoming more frequent and requires more planning for design and optimization tasks, with which it is possible to understand, explain and test without the need to intervene in the actual processes [1]-[7].

Unfortunately, the lack of knowledge about all the phenomena occurring in this type of process is a frequent condition in practice in the mineral processing industry. Such a situation occurs because of the low availability of phenomenological studies and because of some modeling difficulties inherited from past experiences; insufficient computational power induced the false appreciation that phenomenological-based models are complex. The solution of systems of differential equations was the major difficulty faced. This situation was directly reflected in the low availability of accurate models, which caused, for example, design problems in mining-metallurgical processes that had to vary their operating point. Today, it is possible to overcome this difficulty and use models characterized by the need for a large amount of data associated with the operating conditions to predict the behavior of these processes, exploiting the capabilities of the empirical model as the process itself is worked with [1], [6], [7].

Mineral processing is considered fundamental to the mining industry. Classically, the term mineral processing or mineralurgy is used to describe the transformation operations involved in the upgrading and recovery of minerals [8]-[14]. These operations are carried out sequentially to obtain a raw material useful in subsequent processes or a final product desirable in the market. The operations that are grouped under the name mineral processing can be divided into four groups: size reduction, classification, concentration, and refining. Each stands out within a mineralurgical process, according to the mineralogical characteristics of the feed and the specifications of the final product. Concentration uses the difference in physical or volumetric properties of mineral substances for their separation, generating the segregation of two or more species [15], [16]. In a gravimetric concentration equipment, a stream called feed is divided into two: a stream called concentrate, which has a high content of the species of interest and another stream called tails, in which this content is substantially decreased [11], [12], [17]-[24].

Jig is a gravity concentrator device in which mineral particles move relatively in a pulsating water flow resulting in a stratification of particles of different densities and sizes. In Figure-1, a schematic view of a Jig is given. According to Figure-1, we intend to model the dynamics of the separation of high-density minerals from low density minerals in a Jig type gravimetric concentration equipment according to a stratification of the particles present in a feed stream (Fa) whose solids load is less than 10% in volume. The stratification is produced by the transmission of mechanical energy which is generated by the movement of a piston that exerts pressure on the water (F_{h2o}) in the internal chamber of the Jig in a harmonic way, generating a movement in pulses (ascent and descent) of the particulate system that enters the separation chamber of the Jig, so that a stratification of the bed formed by the particles is obtained, which is later used to produce the separation of the minerals. The separation chamber of the Jig is open to the atmosphere, inside it there is a screen where a bed of particles is deposited that have an intermediate density with respect to the minerals to be separated. The particle bed has an initial height H_0 (packed bed) that rises to a height H_{max}, (fully fluidized bed) according to the upward and downward movement of F_{h2o}. The F_{h2o} current contains water at a flow rate greater than or equal to the minimum fluidization velocity of the particles to be separated. The anharmonic motion of F_{h2o} generates a hydrodynamic interaction between the two phases present in the process (solid-solid, solid-liquid interaction). This interaction alters the

movement of the mineral particles present in the separation chamber of the Jig. The upward movement of water and mineral particles is called the fluidization stage. In this stage the mineral particles rise from a height H_0 to a height H_{max}, initiating the stratification of the particles. At the beginning of stratification, the mineral particles with higher density and larger size tend to be deposited in the lower part of the bed, while the particles with lower density and smaller size are located in the upper part of the bed. When the descent stage begins, the denser particles have a higher sedimentation velocity than the less dense particles; this allows that before the compaction of the bed, the heavier mineral particles are deposited quickly below the screen, obtaining after several cycles of pulsation, a complete separation of the mineral particles in two streams: rejection (F_r) and concentrate (F_c). The process is carried out under ambient temperature conditions and no chemical reaction is present.

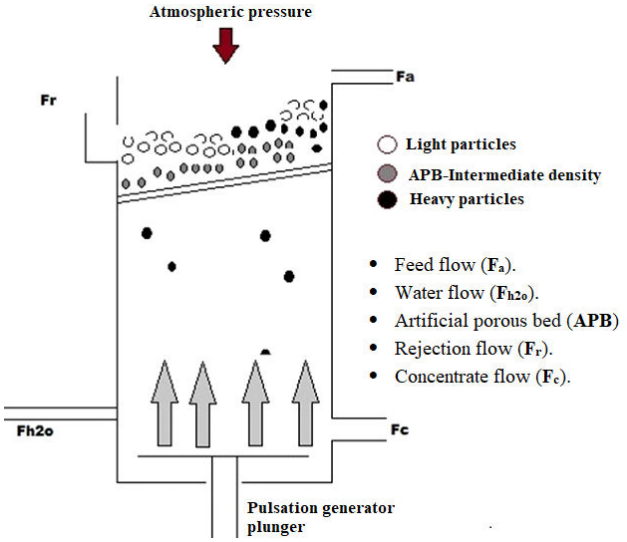

Figure-1. Jig schematic view [20].

According to the above description, particle concentration inside de Jig happens in a complicated multiphase flow system. The separation of particulate species with respect to their specific gravity, through bed height (APB) in gravimetric concentration equipment (see Figure-1), is the result of stratification of suspended particles under the influence of hydrodynamic forces [25]-[30]. Several operational parameters such as water pulsation amplitude and frequency, bed thickness and feed flow characteristics affect the stratification process [31], [32]. The main objective of this paper is to obtain two types of empirical models, autoregressive with exogenous input (ARX) and artificial neural network (ANN), from a set of data obtained from a phenomenological model of the position of a particle inside gravimetric concentration equipment. This model has as input variable, the effect of the solid-fluid interaction force and as perturbation, the solid-solid interaction force. By incorporating the solid-solid and solid-fluid interaction forces into the trajectory model, the particle stratification, and its effect on the recovery in the concentration process can be quantified. The paper gives a detailed description of the formulation of the empirical models, based on the data collected for identification and validation.

The rest of the paper is organized as follows: section two presents the methodology considered for the development of this study through the phenomenological, ARX and ANN models; section three presents the description of model's analysis through discussion of the results obtained; finally, section four presents the conclusions and future work derived from this research.

MATERIAL AND METHODS

The empirical models that will be simulated for the Jig are intended to answer the following question: how is the movement of the particles inside the Jig, with changes in the external variables (frequency and amplitude of the water flow F_{h2o} and mineral solids feed flow F_a)? (These external variables directly affect the trajectory related to the solid-liquid interaction force $F_{S\text{-}L)}$. It is intended to follow the changes in the internal states of the process. As it is a system with strong hydrodynamic interactions, due to the $F_{S\text{-}L}$ interaction force (particle-fluid), the position and linear velocity of the particles would be the internal states or variables of interest.

Phenomenological Model of the Gravimetric Concentrator

The phenomenological model of the gravimetric concentrator considered is based on a mathematical description of solid-solid and solid-fluid interactions. In this model, the force balance on a particle takes into account the effect of continuous variation of the fluid on the particle. Thus, the force balance on a particle in a fluid medium can be expressed by Eq. (1), (2) and (3) [10], [33]-[37].

$$\frac{d^2x}{dt^2} + \frac{\alpha}{m}\frac{dx}{dt} + \frac{\beta}{m}x = \frac{1}{m}F_{S-L} + \frac{1}{m}F_{S-S} \quad (1)$$

$$\alpha = \frac{\mu h}{\varepsilon} \quad (2)$$

$$\frac{\beta}{m} = \bar{\omega}^2 \quad (3)$$

The total force on each particle is composed of the particle-liquid interaction force $F_{S\text{-}L}$ and the particle-particle interaction force $F_{S\text{-}S}$. Eq. (1) represents a non-homogeneous differential equation, where β is the liquid vibration coefficient,$\bar{\omega}^2$ is the undamped natural frequency of vibration, α is the damping coefficient, μ is the liquid viscosity, ε is the bed porosity, h is the bed height at rest, and m is the particle mass.

Eq. (1) describes a second order system, where it can be identified that the particle position x(t) is the output of the system, $F_{S\text{-}L}$ is the input associated to the velocity with which the water drags the particles and $F_{S\text{-}S}$ is a perturbation that is modifying the trajectory of the particles by the collisions between them.

Data Generation for Identification and Validation

In order to obtain sufficient data of the particle position x(t) subject to changes in the input $F_{S\text{-}L}$ and perturbation $F_{S\text{-}S}$ for identification and validation of the empirical models, the particle position is calculated by integrating Eq. (1) by means of the centered difference method where the increments in the position are calculated at each sampling time (t_m =0.02s). Details of the sampling time calculation procedures and the discretization of Eq. (1) can be found in [38]–[43]. Thus, the discretized Eq. (1) takes the form:

$$x_{k+1} = a \cdot x_k - b \cdot x_{k-1} + c \cdot F_{S-L\,k} + d \cdot F_{S-S\,k} \quad (4)$$

$$a = \frac{t_m^2 \cdot \beta + c \cdot t_m + 2 \cdot m}{m + t_m \cdot \alpha} \quad (5)$$

$$b = \frac{m}{m + t_m \cdot \alpha} \quad (6)$$

$$c = d = \frac{t_m^2}{m + t_m \cdot \alpha} \quad (7)$$

The process data are recorded for a total operating time of 10 min.; these data are obtained by perturbing the process by means of random signals. The sequence of the data is shown in Figure-2. The sequence contains 30,000 samples. The input $F_{S\text{-}L}$ is a random signal that varies from a minimum value ($F_{S\text{-}L}$ min=0 mN) to a maximum value ($F_{S\text{-}L}$ max=1.5 mN), and the duration time of the signal is determined to ensure that the excited output does not reach steady states. The duration times were lower than the time where the process reaches its steady state (about 10 s) (maximum duration 8 s) (minimum duration 2 s). The perturbation $F_{S\text{-}S}$ varies randomly in an interval of ±2 mN with maximum and minimum duration times of 13 and 1 s respectively.

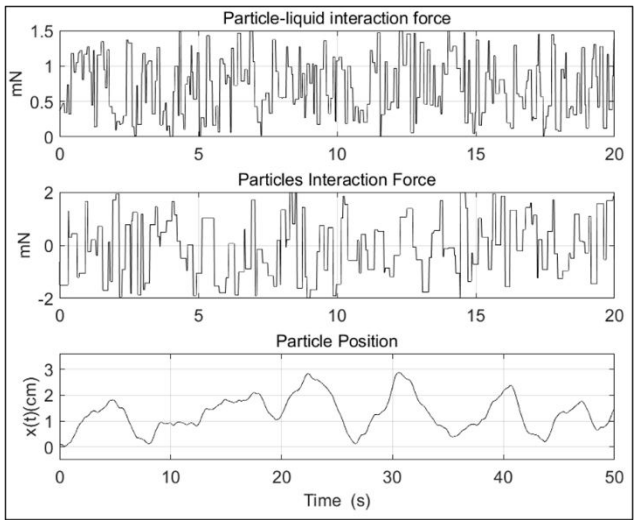

Figure-2. Data used for identification and validation of empirical models.

Once the data is obtained, the time-delay matrix is found (5 time-delays for each variable), this is done in order to get sufficient data for the identification and to ensure which regressors best fit the models. In addition, at this stage of the development it is more convenient to normalize the variables because additional errors corresponding to the physical units of the variables are eliminated. Figure-3 shows the normalized and time-delayed variables.

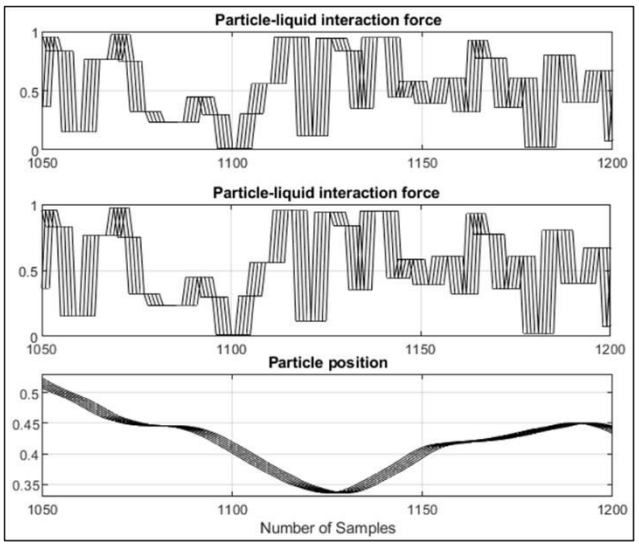

Figure-3. Normalized and time-delayed variables.

With the variables normalized and time-delayed, the data are randomly distributed for identification (training) and validation. According to theory [44]-[51], an adequate division of the data is to take 70% for identification and 30% for validation.

RESULT ANS DISCUSSIÓNS

Particle trajectory patterns that can help to understand the stratification process inside the Jig separation chamber are reviewed. The model was simulated in two software applications, MATLAB®(R2021b) and ANSYS Fluent R2(2020) using a user define function (UDF) to couple the water velocity field and the Runge Kutta method to calculate the particle trajectories, these programs were installed in a computer with a 4-core processor and 8GB of RAM. We used a sampling time t_s=0.01 s.

ARX Model Identification

Using the sequence of identification data (see Figure-3) the X matrix is formed, which contains the regressors and a first column made up of ones, which are used to find the independent term of the ARX model. The matrix is based on adjusting the data by means of least squares algorithm. The following first-order ARX model (see Eq. (8)) was found by performing different simulation tests with the different regressors.

$$x(t) = -5.0678 \times 10^{-4} + 0.9997x(t-1) + \cdots \\ \ldots 5.9027 \times 10^{-4} F_{S-L}(t-4) + \cdots \\ \ldots 6.8411 \times 10^{-4} F_{S-S}(t-5) \quad (8)$$

The order and time-delays for the regressors of the ARX model in Eq. (8) were determined by means of a step test to the system, showing a reasonable fit with respect to the other simulations with the identification data.

ANN Model Identification

Since the objective is to compare the performance of both types of models, the same regressors that were used in the identification of the ARX model should be used for the identification of the ANN model. A multilayer perceptron ANN with three inputs (corresponding to the three regressors used) was created using the Matlab® artificial neural network toolbox. The program identifies the three input regressors and the output. From the simulations performed, errors of less than 2% were obtained with 5 neurons in the hidden layer and starting the training process for 10 epochs. The results of the network without training and the training performance are shown in Figures 4 and 5 respectively.

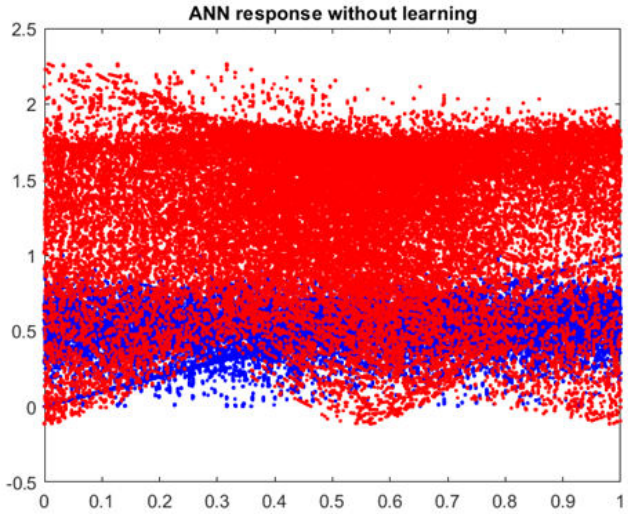

Figure-4. Network performance without learning.

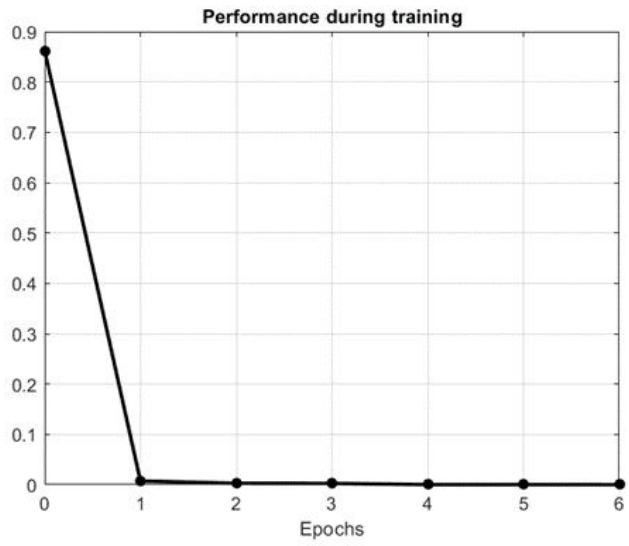

Figure-5. Learning performance.

Figure-4 shows the unsorted distribution of the data for the untrained neural network, once the training algorithm is started, it converges in only 4 epochs (see Figure-5), making the network follow the input patterns that have been provided.

Discussion of the Identification and Validation Results

The performance of the two identified models was compared in two stages. In the first stage Figures 6 and 7, the identification data are shown with the absolute errors (maximum, average and minimum) that are reported in Table-1.

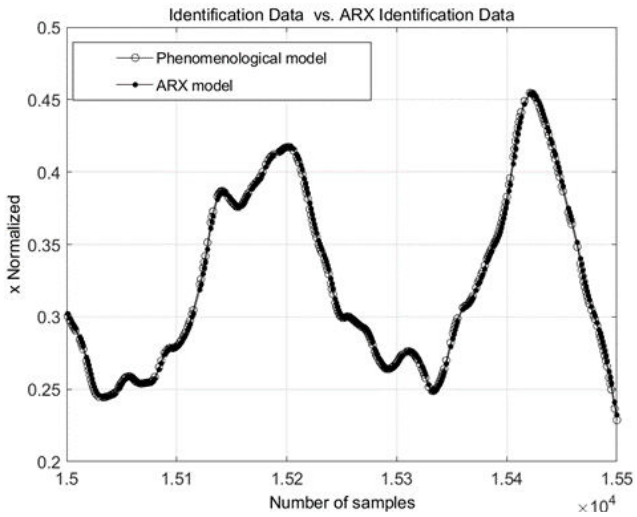

Figure-6. ARX model simulation based on the identification data.

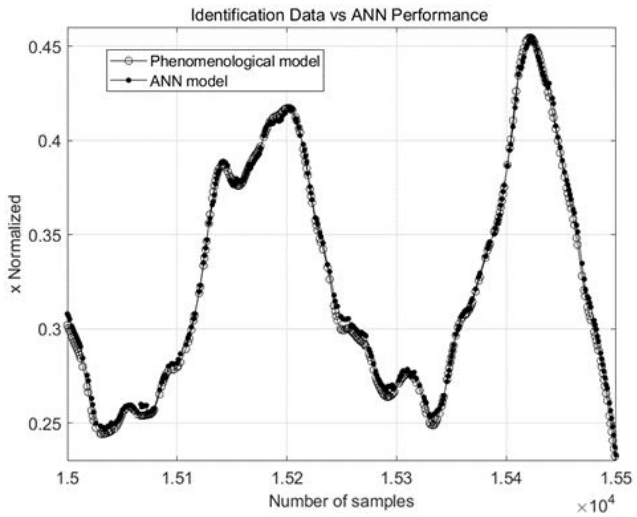

Figure-7. ANN model simulation based on the identification data.

Table-1. Absolute errors in identification.

Model	Max. Error (%)	Mean Error (%)	Min. Error (%)
ARX	1.06	0.23	1.64x10-5
ANN	1.27	0.34	6.03x10-6

In the second stage the models are compared by means of the validation data (Figures 8 and 9) with their respective absolute errors presented in Table-2.

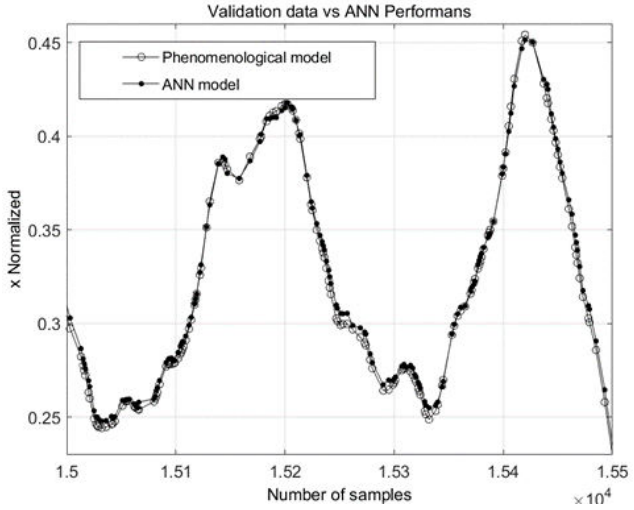

Figure-8. ARX model simulation based on the validation data.

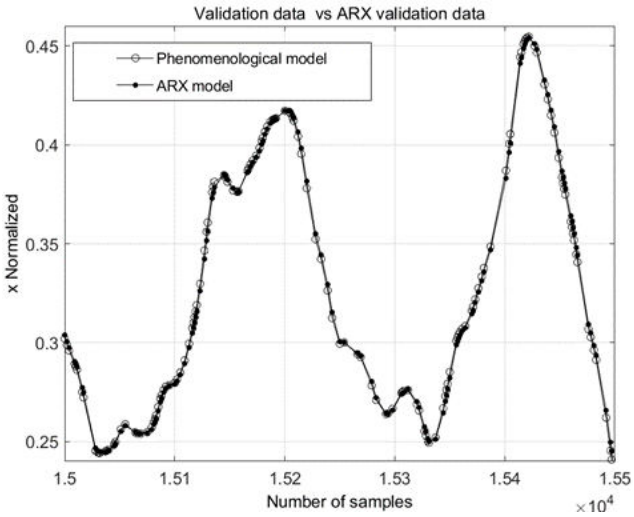

Figure-9. ANN model simulation based on the validation data.

Table-2. Absolute errors in validation.

Model	Max. Error (%)	Mean Error (%)	Min. Error (%)
ARX	1.03	0.22	3.37×10^{-5}
ANN	1.22	0.34	1.47×10^{-6}

It can be seen from Figures 6 to 9 and Tables 1 and 2 that the performance of both models is good, both in identification and validation, yielding errors of less than 2%, which is adequate for engineering purposes, especially to implement a control strategy for the Jig concentration process.

Comparing the errors of both models, it can be said that the performance of the ARX model is somewhat better than the performance of the ANN model. This may be due to the fact that regressors from the ARX model are used to train the ANN model for comparison purposes. The error in the ANN model could be decreased by two orders of magnitude if more regressors were chosen from the time-delay matrix ordelve into the number of neurons and hidden layers in the network that give a better fit with respect to the data provided.

The prediction performance of the two identified models is compared by simulations with the validation data (see Figures 8 and 9). It is evident that the ARX model performs better than the ANN model. Note that, since the validation data were recorded from a mathematical model and not from experimental data, it is necessary to be able to validate both models taking into account the environmental conditions as there could be a significant, but constant, offset between the simulation result and the recorded data. This type of drawback is easily compensated with an integral action in a controller.

The average prediction errors that were estimated using the validation data sequence for the two models are shown in Table-2. We see that the ARX model performs somewhat better than the ANN model. The prediction errors reveal that a significant amount of dynamics remains unmodeled. This may be due to the slow time constant that we have neglected and other effects that have not been adequately modeled in the phenomenological mathematical structure.

CONCLUSIONS

In this work, two empirical models were developed, and their performance was evaluated by means of absolute errors. It can be said that the application of empirical models to the study of dynamic systems is very limited, since they are highly dependent on the operating conditions, any change in the process variables makes the model deviate significantly, causing a bad performance on the real processes.

It is concluded from the simulations performed that the ANN model is very sensitive to the data provided. Further simulations on the ANN model, changing the number of regressors and the number of neurons in the hidden layer, show very significant changes in the errors of the identification and validation data.

This paper has shown that the modeling framework based on local models and interpolation may give models that are as useful, accurate, and reliable as with phenomenological modeling, even if the system is well understood. Such models may serve as an alternative that may be attractive especially for systems that are not well understood, as in the case of Jig. Moreover, we believe empirical models developed in this framework have significant advantages over many other non-linear empirical modeling frameworks. The reason is that it admits interpretability of the model through the intuitive and easily understandable operating regime concept, and the fact that the local ARX models can be interpreted independently.

ACKNOWLEDGMENTS

Authors are grateful for the support of simulations works by project "Diseño y modelamiento de un concentradorgravimétrico con campo eléctrico para la recuperación de minerals" with ID P20221. Materiales Avanzados y Energía (MATYER) and Automática y Electrónica groups at the Instituto Tecnológico Metropolitano, Medellín-Colombia, and the Systems Engineering program of the Universidad de Cartagena, for their support in the financing, use of equipment and advice provided by the researchers.

REFERENCES

[1] H. Alvarez, R. Lamanna, P. Vega and S. Revollar. 2009. Methodology for Obtaining Phenomenological-Based Semiphysical Models applied to a Sugar Cane Sulfitation Tower (in Spanish). Rev. Iberoam. Automática e Informática Ind. RIAI, 6(3): 10-20, doi: 10.1016/S1697-7912(09)70260-2.

[2] K. Hangos and I. Cameron. 2001. Process modelling and model analysis. London.

[3] E. Hoyos, D. López and H. Alvarez. 2016. A phenomenologically based material flow model for friction stir welding. Mater. Des. 111: 321-330, doi: 10.1016/j.matdes.2016.09.009.

[4] L. Lema, R. Muñoz, J. Garcia and H. Alvarez. 2018. On parameter interpretability of phenomenological-based semiphysical models in biology. Informatics Med. Unlocked, 15(November 2018): 100158, doi: 10.1016/j.imu.2019.02.002.

[5] L. Lema-Perez, J. Garcia-Tirado, C. Builes-Montaño, and H. Alvarez. 2019. Phenomenological-Based model of human stomach and its role in glucose metabolism. J. Theor. Biol., 460: 88-100, doi: 10.1016/j.jtbi.2018.10.024.

[6] S. López and C. Zuluaga. 2013. Modelo semifísico de base fenomenológica de un evaporador de jugo de caña de azucartipo Roberts. Ingenio Magno. 4: 32-38.

[7] C. C. Zuluaga, M. Ruiz, M. A. Ospina and J. F. Garcia. 2018. A dynamical model of an aeration plant for wastewater treatment using a phenomenological based semi-physical modeling methodology. Comput. Chem. Eng., 117: 420-432, doi: 10.1016/j.compchemeng.2018.07.008.

[8] A. Andalusite *et al*. 2001. Composition and specific gravities of some common minerals. Model. Simul. Miner. Process. Syst., pp. 395-397, doi: 10.1016/b978-0-08-051184-9.50015-8.

[9] K. Asakura, M. Mizuno, M. Nagao and S. Harada. 2007. Numerical Simulation of Particle Motion in a Jig Separator. in 5th Join ASME JSME Fluids Engineering Conference. pp. 385-391.

[10] K. Asakura, S. Harada, T. Funayama and I. Nakajima. 1997. Simulation of descending particles in water by the distinct element method. Powder Technol. 94: 195-200.

[11] R. Burt. 1999. The role of gravity concentration in modern processing plants. Miner. Eng. 12(11): 1291-1300.

[12] R. Burt and C. Mills. 1984. Gravity concentration technology, Vol 5. Amsterdam, Netherlands: Elsevier.

[13] D. W. Fuerstenau and Pradip. 2005. Zeta potentials in the flotation of oxide and silicate minerals. Adv. Colloid Interface Sci., 114-115: 9-26, doi: 10.1016/j.cis.2004.08.006.

[14] R. P. King. 2001. Simulation of Ore Dressing Plants. in Modeling and Simulation of Mineral Processing Systems. pp. 351-394.

[15] B. A. Wills, Minerals Processing Technology. London: Butterworth-Heinemann, 1997.

[16] R. P. King. 2001. Solid-liquid separation. in Modeling and Simulation of Mineral Processing Systems. pp. 213-231.

[17] W. M. Ambrós. 2020. Jigging: A review of fundamentals and future directions. Minerals, 10(11): 1-29, doi: 10.3390/min10110998.

[18] W. M. Ambrós, C. H. Sampaio, B. G. Cazacliu, P. N. Conceição and G. S. dos Reis. 2019. Some observations on the influence of particle size and size distribution on stratification in pneumatic jigs. Powder Technol., 342: 594-606, doi: 10.1016/j.powtec.2018.10.029.

[19] W. M. Ambrós, C. H. Sampaio, B. G. Cazacliu, G. L. Miltzarek and L. R. Miranda. 2017. Usage of air jigging for multi-component separation of construction and demolition waste. Waste Manag., 60: 75-83, doi: 10.1016/j.wasman.2016.11.029.

[20] M. O. Bustamante, A. C. Gaviria and O. J. Restrepo. 2008. Class notes of the subject: minerals

Concentration. Medellín: Universidad Nacional de Colombia-sede Medellín.

[21] M. A. Ospina. 2014. Modelamiento de la hidrodinámica de la separación gravimétrica de minerales en jigs. Universidad Nacional de Colombia.

[22] M. A. Ospina and M. O. Bustamante. 2015. Hydrodynamic study of gravity concentration devices type JIG. Rev. Prospect., 13(1): 52-58, doi: http://dx.doi.org/10.15665/rp.v13i1.359.

[23] M. A. Ospina, A. B. Barrientos and M. O. Bustamante. 2016. Influence of the pulse wave in the stratification of high-density particles in a JIG device. Rev. Tecno Lógicas. 19(36): 13-25.

[24] M. A. Ospina and L. M. Usuga. 2018. Effect of Hydrodynamic forces on mineral particles trajectories in Gravimetric concentrator Type Jig. Politecnica. 14(27): 68-79.

[25] L. C. Woollacott. 2019. The impact of size segregation on packing density in jig beds: An X-ray tomographic study. Miner. Eng., 131(June 2018): 98-110, doi: 10.1016/j.mineng.2018.10.017.

[26] S. Viduka, Y. Feng, K. Hapgood and M. Schwarz. 2012. CFD-DEM investigation of particle separations using a Trapezoidal jigging profile. in Ninth International Conference on CFD in the Minerals and Process Industries, pp. 1-8, doi: 10.1016/j.apt.2012.11.012.

[27] S. Viduka, Y. Feng, K. Hapgood and M. Schwarz. 2013. Discrete particle simulation of solid separation in a jigging device. Int. J. Miner. Process. 123: 108-119, doi: 10.1016/j.minpro.2013.05.001.

[28] S. Viduka, Y. Feng, K. Hapgood and P. Schwarz. 2013. CFD-DEM investigation of particle separations using a sinusoidal jigging profile. Adv. Powder Technol., 24(2): 473-481, doi: 10.1016/j.apt.2012.11.012.

[29] L. C. Woollacott, M. Bwalya and L. Mabokela. 2015. A validation study of the King stratification model. J. South. African Inst. Min. Metall., 115(2): 93-101, doi: 10.17159/2411-9717/2015/v115n2a2.

[30] L. C. Woollacott and M. Silwamba. 2016. An experimental study of size segregation in a batch jig. Miner. Eng., 94: 41-50, doi: 10.1016/j.mineng.2016.04.003.

[31] F. Pita and A. Castilho. 2016. Influence of shape and size of the particles on jigging separation of plastics mixture. Waste Manag., 48: 89-94, doi: 10.1016/j.wasman.2015.10.034.

[32] E. F. Crespo. 2016. Modeling segregation and dispersion in jigging beds in terms of the bed porosity distribution. Miner. Eng., 85: 38-48, doi: 10.1016/j.mineng.2015.10.012.

[33] K. Asakura, M. Nagao and M. Mizuno. 2007. Simulation of Particle Motion in a Jig Separator. J. JSEM, 7(Special Issue).

[34] S. Cierpisz. 2017. A dynamic model of coal products discharge in a jig. Miner. Eng., 105: 1-6, doi: 10.1016/j.mineng.2016.12.010.

[35] C. Coimbra and R. Rangel. 1998. General solution of the particle momentum equation in unsteady Stokes flows. J. Fluid Mech., 370: 53-72, doi: doi: 10.1017/S0022112098001967.

[36] R. King. 2001. Gravity separation. in Modeling and Simulation of Mineral Processing Systems. pp. 233-267.

[37] B. K. Mishra and S. P. Mehrotra. 2001. A jig model based on the discrete element method and its experimental validation. Int. J. Miner. Process. 63: 177-189, doi: 10.1016/S0301-7516(01)00053-9.

[38] S. Cierpisz. 1984. Some Aspects of the Optimal Control of the Coal Separation Process. IFAC Proc. Ser., 16(15): 445-455, doi: 10.1016/s1474-6670(17)64298-8.

[39] S. Cierpisz and E. Jachnik. 1987. On Optimal Control of Coal Separation Process. IFAC Proc. 20(8): 123-127, doi: 10.1016/s1474-6670(17)59081-3.

[40] S. Cierpisz and J. Joostberens. 2016. Monitoring of coal separation in a jig using a radiometric density meter. Meas. J. Int. Meas. Confed., 88: 147-152, doi: 10.1016/j.measurement.2016.03.060.

[41] S. Cierpisz, M. Kryca, and W. Sobierajski. 2016. Control of coal separation in a jig using a radiometric meter. Miner. Eng., 95: 59-65, doi: 10.1016/j.mineng.2016.06.014.

[42] G. J. Lyman. 1992. Review of Jigging Principles and Control. Coal Prep., 11(3-4): 145-165, doi: 10.1080/07349349208905213.

[43] R. Rong and G. Lyman. 1991. Modelling jig bed stratification in a pilot scale baum jig. Miner. Eng. 4(5-6): 611-623.

[44] L. He, K. Wen, C. Wu, J. Gong and X. Ping. 2020. Hybrid method based on particle filter and NARX for real-time flow rate estimation in multi-product pipelines. J. Process Control, 88: 19-31, doi: 10.1016/j.jprocont.2020.02.004.

[45] T. A. Johansen and B. Foss. 1993. Constructing NARMAX models using ARMAX models. Int. J. Control, 58(5): 1125-1153, doi: 10.1080/00207179308923046.

[46] M. Lin, C. Cheng, Z. Peng, X. Dong, Y. Qu and G. Meng. 2021. Nonlinear dynamical system identification using the sparse regression and separable least squares methods. J. Sound Vib, 505: 116141, doi: 10.1016/j.jsv.2021.116141.

[47] L. Ljung and T. Glad. 1994. Modeling of dynamic systems. New Jersey: Englewood Cliff.

[48] M. Sugeno and T. Takagi. 1985. Fuzzy identification of systems and its applications to modeling and control. IEEE Trans. Syst. Man. Cybern. 15(1): 116-132.

[49] T. Zhang, R. J. Barthorpe and K. Worden. 2020. On Treed Gaussian Processes and piecewise-linear NARX modeling. Mech. Syst. Signal Process, 144: 106877, doi: 10.1016/j.ymssp.2020.106877.

[50] M. Zheng and Y. Ohta. 2021. Bayesian positive system identification: Truncated Gaussian prior and hyperparameter estimation. Syst. Control Lett. 148: 104857, doi: 10.1016/j.sysconle.2020.104857.

[51] S. A. Zulkeflee, F. S. Rohman, S. Abd Sata and N. Aziz. 2021. Autoregressive exogenous input modelling for lipase catalysed esterification process. Math. Comput. Simul. 182: 325-339, doi: 10.1016/j.matcom.2020.11.006.